The adsorption of methyl nitrite on the Au(111) surface

J.R.B. Gomes and F. Illas *

Departament de Química Física i Centre de Recerca en Química Teòrica, Universitat de Barcelona, C/ Martí i Franquès 1, E-08028 Barcelona, Spain
E-mail: f.illas@qf.ub.es

Received 13 July 2000; accepted 31 October 2000

The interaction of the methyl nitrite molecule (CH_3ONO) with the gold(111) surface has been studied by means of density functional calculations. The perfect Au(111) surface has been represented by a rather large cluster model, Au_{22}, that was in turn used to extract information about the preferred adsorption geometry of the CH_3ONO species. Vibrational frequencies and adsorption energy are also reported. The calculated adsorption energies are 31.2 kJ/mol with respect to gas phase *cis*-conformer and 35.1 kJ/mol with respect to *trans*-methyl nitrite, very close to the experimental adsorption energy of 33.5 kJ/mol. From the analysis of vibrational frequencies of gas phase and adsorbed species it is concluded that only the *cis*-conformer is present at the Au(111) surface.

KEY WORDS: methyl nitrite; density functional theory; Au(111); chemisorption; vibrations of adsorbed species

1. Introduction

Methyl nitrite (CH_3ONO) has been proposed as an intermediate in the homogeneous [1] decomposition of nitromethane (CH_3NO_2) and could be present also in the heterogeneous reaction. The adsorption of this species is of interest since methyl nitrite has a weak CH_3O–NO bond (42 kcal/mol in the gas phase [1]) and therefore it can be used as an adsorbed precursor for preparing surface methoxy species. Also, the importance of nitromethane as one of the simplest explosives and as a monopropellant in rocket thrusters make these species a model to more complex molecules. Numerous experimental as well as theoretical studies concerning methyl nitrite reactions as a reactant or an intermediate species can be found in the literature [1–11]. However, most of the existing studies are related to gas phase chemistry [1–7], and only a few works are devoted to the adsorbed methyl nitrite molecule on heterogeneous catalysts [8–11].

Koel and co-workers have studied the CH_3ONO adsorption on Au(111) [8], Pt–Sn [9] and on Pt(111) [10] surfaces. On Au(111), the authors propose that adsorbed methyl nitrite exists both in the *cis* and *trans* forms with the O–N–O group in a flat lying geometry nearly parallel to the surface. Pressley et al. [11] studied the methyl nitrite surface chemistry on the Ag(111) surface and their data suggest a geometry in which lone-pair electrons on the internal oxygen atom, and possibly on the nitrogen atom, donate electron density towards the surface. A geometry where the C–O–N plane is tilted away from the surface normal both in *cis* and *trans* forms of CH_3ONO is also proposed. A larger interaction of the central oxygen atom with the metal surface is consistent with the propensity to eject NO when either electrons or phonons activate adsorbed CH_3ONO [11]. Temperature-programmed desorption (TPD) data obtained in ultrahigh vacuum (UHV) conditions show a very different behavior for CH_3ONO on these four surfaces. On Ag(111) and on Au(111), no thermal reaction was observed. On the other hand, on Pt(111) and on Pt–Sn alloys CH_3ONO is decomposed to NO and an intermediate, possibly CH_3O, which subsequently transforms to CH_3OH or CO and H_2 on the perfect Pt surface and to H_2CO on Pt–Sn surface alloys. In a very recent work, concerning the photodissociation of *t*-butyl nitrite, $(CH_3)_3CONO$, on the Ag(111) surface, an orientation where both oxygen atoms interact with the surface (*trans* form) via the lone-pair electrons is proposed [12].

The difficulties in the interpretation of experimental data in these systems are clearly described in [13] and references therein. In particular, difficulties arising from the interpretation of experimental data concerning the geometry of the CH_3ONO species on metal surfaces are evidenced in [8,11]. The structures for *cis*- and *trans*-methyl nitrite adsorbed on the Au(111) surface [8] differ significantly from those proposed on the Ag(111) surface [11]. First, the *trans* form suggested in [8], figure 1(a), for adsorption on the gold surface has the O–N=O group in an flat lying geometry while the structure proposed for the silver surface [11], figure 1(b), has the C–O–N plane parallel to the surface and the N=O bond in an upright conformation. Secondly, the *cis* form proposed in [8], figure 1(c), is expected to suffer from a large steric effect destabilization due to the proximity between the methyl group, the O–N=O group and the metal surface. From ultraviolet photoelectron spectroscopy (UPS), work-function change measurements ($\Delta\Phi$) and X-ray photoelectron spectroscopy data, a geometry in which the central oxygen atom interacts with the surface and possibly the nitrogen atom too is also suggested [11], figure 1(d). In a certain manner this suggestion contradicts the adsorption schemes presented by these authors in the same paper [11] where the nitrogen atom

* To whom correspondence should be addressed.

1011-372X/01/0100-0031$19.50/0

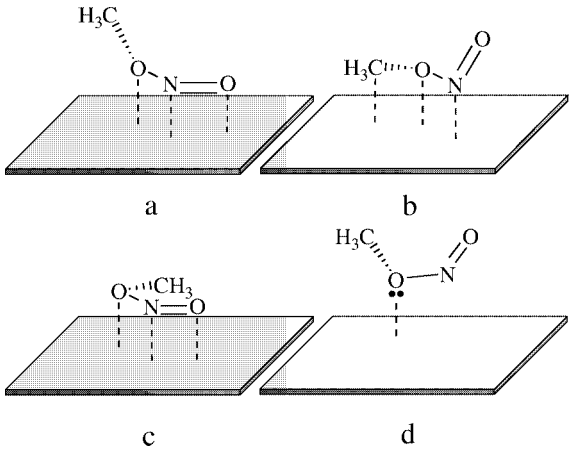

Figure 1. Experimentally proposed adsorption schemes for methyl nitrite on Ag and Au(111) surfaces. *Trans*-conformer adsorbed on (a) Au(111) and (b) Ag(111). *Cis* form on (c) Au(111) and on (d) Ag(111).

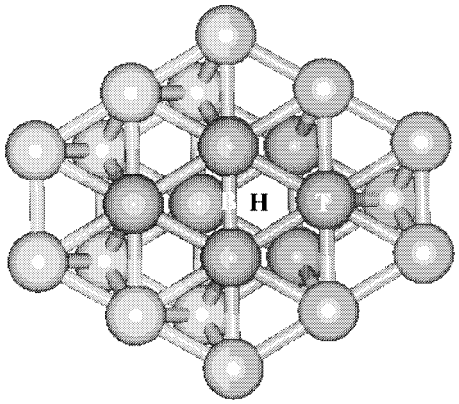

Figure 2. Top view of the Au_{22} (14,8) cluster used to model the (111) gold surface. B, H and T label the three different bridge, hollow and top adsorption sites, respectively.

is shown to lie much closer to the surface than the oxygen atom. Significant differences between methyl nitrite adsorption on Ag(111) and Au(111) surfaces are not expected since previous studies [14,15] show that the main difference between adsorption on silver and on gold concerns mainly the interaction energies. The adsorption energy is larger for the Ag surface than for the Au surface and the geometric parameters are similar.

2. Computational details

In the present work, the cluster model approach [16,17] together with density functional theory (DFT) based calculations have been used to investigate the adsorption geometry of methyl nitrite adsorbed on the Au(111) surface. The DFT calculations were carried out by means of the B3LYP hybrid method which yields very good results in systems where transition metal atoms are present [18–23]. The hybrid B3LYP method uses an exchange functional that mixes the non-local Fock exchange with the gradient corrected form proposed by Becke [24] and adds the functional correlation proposed by Lee et al. [25] based in the previous work of Colle and Salvetti [26,27]. To model the metal surface, the Au_{22} cluster model depicted in figure 2 has been used. This reasonably large cluster with C_s symmetry is made up of two metal layers. The first metal layer contains fourteen gold atoms and the second layer contains eight metal atoms. A third layer was judged to be unnecessary because of the local nature of the chemisorption phenomena and vibrational frequencies. In order to make the calculations feasible the gold atoms in the cluster model were assigned to different regions that are treated differently in terms of basis set employed. The Au atoms closest to the adsorption site, four from the outer layer and three from the second layer, define the inner region. The atoms in this region were treated with the LANL2DZ basis set derived by Hay and Wadt [28]. This basis set treats explicitly the outer $5s^25p^65d^{10}6s^1$ electrons in gold atoms by a double-zeta basis set while the inner core electrons were replaced by the relativistic effective core potential, RECP, of Hay and Wadt [28]. The gold atoms farther from the adsorption site, outer region, were described by the LANL2MB [28] basis set which differs from the LANL2DZ basis set by the use of a minimal basis instead of the double-zeta one to treat the valence electrons. These two different regions are illustrated in figure 2. The standard split valence basis set, 6-31G, plus polarization and diffuse functions, resulting in a 6-31+G* basis, has been employed to describe the non-metallic atoms. All calculations were carried out by means of the Gaussian 98 suite of programs [29].

3. Results and discussion

The computed geometries and energies for the gas phase *cis* and *trans* conformations of methyl nitrite are compared to previous calculated [30] and experimental microwave spectra results [31,32] in table 1. For the *cis*-methyl nitrite, the results obtained with the B3LYP/6-31+G* approach compare to experiment even better than those obtained using the in principle more accurate, and much more computing resources demanding, CCSD(T)/6-311++G(2d,2p) method [30]. The largest deviations between B3LYP results and experimental values correspond to the C–O bond length and the C–O–N angles. Likewise, results presented in this work for the *trans*-methyl nitrite molecule also agree with available experimental data. Again, B3LYP plus the 6-31+G* basis set shows to be competitive when compared with the coupled-cluster including triple excitations results. For the angle between the methyl hydrogen atom in the molecular plane and the C–O bond, see figure 3, a curious difference between B3LYP and CCSD(T) results occurs. The B3LYP predicts a value of $\sim 105^\circ$ close to the experimental value from [31] while the CCSD(T) result of 109.6° close to the experimental value reported in [32]. The energetic results show that *cis*-methyl nitrite is more stable than the *trans*-conformer. The energy difference between both isomers is $\sim$4 kJ/mol while using either B3LYP/6-31+G* or CCSD(T)/6-311++G(2d,2p). Again, the B3LYP/6-31+G*

Table 1
Geometric parameters and total energy for *cis*- and *trans*-conformers of methyl nitrite calculated using the B3LYP method plus the and 6-31+G* basis set. Results are compared to CCSD(T)/6-311++G(2d,2p) theoretical values [23] and microwave spectra experimental results [24,25]. In bold, the results calculated in this work that when compared to CCSD(T) values agree better with experimental data.

Parameter	*Cis*-methyl nitrite			*Trans*-methyl nitrite		
	B3LYP 6-31+G*	CCSD(T) 6-311++G(2d,2p)	Experimental [25]	B3LYP 6-31+G*	CCSD(T) 6-311++G(2d,2p)	Experimental [24] ([25])
d(N=O) (Å)	**1.1908**	1.1933	1.182	1.1821	1.1772	1.170 (1.164)
d(O–N) (Å)	**1.3963**	1.4011	1.398	1.4125	1.4323	1.451 (1.415)
d(C–O) (Å)	1.4426	1.4369	1.437	1.4405	1.4379	1.435 (1.436)
d($H_{1,2}$–C) (Å)	**1.0941**	1.0848	1.102	**1.0940**	1.0862	1.099 (1.09)
d(H_3–C) (Å)	**1.0899**	1.0800	1.09	**1.0908**	1.0875	1.099 (1.09)
d(C···O) (Å)	2.5349	–	–	–	–	–
∠ (O–N=O) (deg.)	**114.57**	114.41	114.8	**110.99**	111.05	110.2 (111.8)
∠ (C–O–N) (deg.)	116.08	114.09	114.7	110.20	109.33	107.8 (109.9)
∠ ($H_{1,2}$–C–O) (deg.)	**110.56**	110.67	109.9	**110.59**	108.52	111.0 (109.5)
∠ (H_3–C–O) (deg.)	**104.23**	104.44	101.8	**105.05**	109.62	102.6 (109.5)
∠ ($H_{1,2}$–C–O–H_3) (deg.)	**119.22**	119.34	118.8	**118.68**	120.16	118.1 (120.0)
∠ (H_1–C–O–H_2) (deg.)	**121.54**	121.32	122.4	**122.64**	119.68	123.8 (120.0)
Energy (a.u.)	−245.015772	−244.656520	–	−245.014293	−244.654913	–

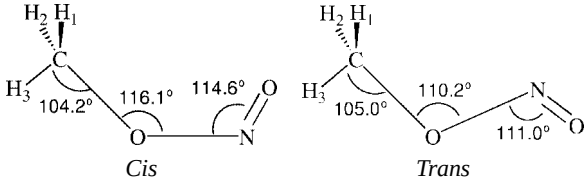

Figure 3. Gas phase optimised structures for *cis*- and *trans*-methyl nitrite.

Table 2
Calculated geometrical parameters for gas phase *cis*-methyl nitrite and adsorbed on the Au(111) surface. d – distance, nn$d$ – distance to the nearest gold atom in the surface, ∠ – bond or dihedral angles.

Geometrical parameters	CH_3ONO adsorbed on Au(111)[a]	Free *cis*-CH_3ONO[a]
d(N=O) (Å)	1.1920	1.1908
d(O–N) (Å)	1.3922	1.3963
d(C–O) (Å)	1.4426	1.4426
d($H_{1,2}$–C) (Å)	1.0941	1.0941
d(H_3–C) (Å)	1.0897	1.0899
d(C···O) (Å)	2.5435	2.5349
nn$d$(O–Au) (Å)	3.5591	–
nn$d$(N–Au) (Å)	4.1938	–
nn$d$(C–Au) (Å)	4.2078	–
nn$d$(H_3–Au) (Å)	3.2645	–
Tilt (O–N) (deg.)	32.82	–
Tilt (C–O) (deg.)	30.59	–
∠ (O–N=O) (deg.)	114.65	114.57
∠ (C–O–N) (deg.)	116.59	116.08
∠ ($H_{1,2}$–C–O) (deg.)	110.44	110.56
∠ (H_3–C–O) (deg.)	104.14	104.23
∠ ($H_{1,2}$–C–O–H_3) (deg.)	119.22	119.22
∠ (H_1–C–O–H_2) (deg.)	121.56	121.54
∠ (H_1–C–O–H_2) (deg.)	121.56	121.54

approach shows to be competitive with more computational resources demanding methods.

The starting adsorption sites used for methyl nitrite adsorbed on the Au(111) surface are shown in figure 2. Labels T, B and H mean adsorption of the *cis*-methyl nitrite with the central oxygen atom placed above a top, bridge and

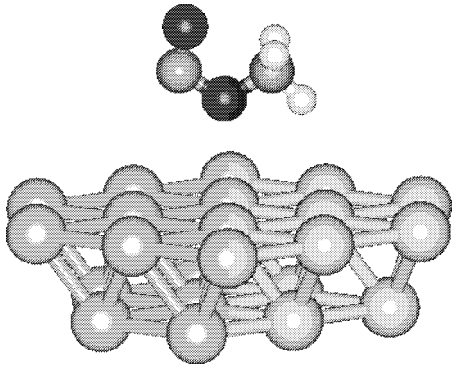

Figure 4. Side view of the final optimised structure of methyl nitrite adsorbed on the Au_{22} (14,8) cluster shown in figure 1. The central oxygen atom of the adsorbed CH_3ONO molecule is located above the bridge site connecting two neighbouring gold atoms.

hollow site, respectively. Based on experimental information [8,11], the optimization of the adsorbate geometry has been carried out starting from an orientation where the O–N axis is parallel to the surface. Next, all parameters defining the internal geometry of CH_3ONO and their position above the surface have been fully optimized, keeping the cluster geometry fixed at the bulk value. Despite the fact that different initial conformations were used, the energy gradient driven optimization procedure always converges to the same final structure. In this optimum geometry, the central oxygen atom is always placed above the bridge site but the O–N bond is considerably tilted away from the surface. This final geometry clearly indicates that the interaction occurs through an oxygen lone pair. The optimized geometric parameters for the final structure are reported in table 2 and in figure 4.

The calculated equilibrium geometry for the adsorbed species is very similar to those calculated for the gas phase *cis*-methyl nitrite. Differences in internal bond lengths are smaller than 0.01 Å and than 0.6° for bond and dihedral angles. The C–O and O–N bonds are tilted away from

the parallel to the metal surface leaving the central oxygen atom much closer to the surface when compared to the carbon and nitrogen atoms. The oxygen atom lies 3.6 Å away from the nearest surface gold atom while carbon and nitrogen are 4.2 Å displaced from the nearest gold atoms, cf. table 2. The C–O and N–O bonds tilting angles from the parallel to the Au(111) surface are 30.6° and 32.8°, respectively. From the low adsorption energy of 33.5 kJ/mol reported experimentally [8], the similarity between the internal geometry of adsorbed and gas phase CH_3ONO is to be expected. Present calculations show that this is indeed the case. The calculated interaction energy is defined as the negative difference between the energy of the metal cluster plus the adsorbate at the optimum geometry minus the energy of the separated fragments. Hence, a calculated value of 31.2 kJ/mol with respect to separated *cis*-methyl nitrite is found, this in turn being 35.1 kJ/mol when referred to the *trans*-conformer. Therefore, the CH_3ONO adsorption energy should lie between 31.2 and 35.1 kJ/mol since in the gas phase a mixture of both conformations exists. The calculated value for the interaction energy is surprisingly close to the experimental result. Given the rather limited representation of the surface, the agreement between theoretical and experimental interaction energies is perhaps fortuitous. Nevertheless, it is concluded that, as predicted by Pressley et al. [11] for the methyl nitrite adsorption on the Ag(111) surface, the interaction of CH_3ONO with the metal surface arises essentially from the oxygen lone-pair electrons, the adsorbate donates electronic density towards the metal surface. On the other hand, the larger distance to the surface calculated for the carbon and nitrogen atoms is in agreement with experimental evidence arising from the activation of the CH_3ONO adsorbed molecule by electrons or phonons [11]. Under these conditions the surface ejects NO molecules to the gas phase and leads to an adsorbed methoxy species that is known to bond metal surfaces through the oxygen atom [14,33]. It is worth pointing out that the calculated adsorption geometry described above is also in agreement with the model suggested in [11]. These authors found a monolayer-coverage ratio of one CH_3ONO molecule per three surface atoms. A possible adsorption scheme compatible with these measurements is given in figure 5. Due to the large surface area occupied by the adsorbed methyl nitrite molecule, the possible neighboring adsorption sites in the COM plane direction and in oblique directions would be not available for adsorption because of the large steric hindrance.

Vibrational frequencies for the adsorbed CH_3ONO species were also calculated and are reported in table 3. Selected computed vibrational frequencies for *cis*-CH_3ONO adsorbed on the Au(111) surface are compared in table 3 to those computed for the two conformers in the gas phase, using the same computational approach, to the HREELS values for CD_3ONO adsorbed on the Au(111) surface [8] and to the FTIR values for solid CH_3ONO [34]. Since there are no

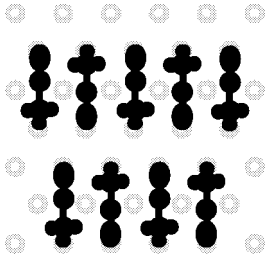

Figure 5. Possible packing arrangement of methyl nitrite on (111) metal surfaces with a monolayer-coverage ratio of one CH_3ONO molecule per three metal surface atoms. In black the aligned CH_3ONO molecules and in light grey the Au(111) surface top layer.

Table 3
Vibrational frequencies for adsorbed *cis*-methyl nitrite on the Au(111) surface. Results for the free *cis*- and *trans*-conformers are also reported.

Vibrational frequencies	CH_3ONO adsorbed on Au(111)[a]	Free *cis*-CH_3ONO[a]	Free *trans*-CH_3ONO[a]	CD_3ONO monolayer on Au(111)[b]	Solid *cis*-CH_3ONO[c]
$\nu_{as}(CH_3)$	3189	3192	3180	2275	3031
$\nu_{as}(CH_2)$	3145	3145	3146	–	3001
$\nu_s(CH_3)$	3068	3070	3067	–	2952
ν(N=O)	1684	1690	1754	1635	1613
$\delta_{as}(CH_3)$	1503	1507	1516	–	1454
$\delta_{as}(CH_3)$	1503	1496	1507	–	1438
$\delta_s(CH_3)$	1451	1455	1474	1050	1408
$\rho(CH_3)$	1191	1192	1204	–	1230
$\rho(CH_3)$	1160	1160	1174	–	1140
ν(C–O)	1001	1002	1057	945	990
ν(O–N)	859	861	845	790	838
δ(O–N–O)	690	681	597	585	625
τ(O–NO)	372	369	350	–	–
δ(C–O–N)	342	343	211	310	351
$\tau(CH_3$–O)	185	186	xxx i	–	–

[a] B3LYP/6-31+G*.
[b] HREELS results taken from [8].
[c] FTIR values taken from [26].
[d] TPD result taken from [8].

significative differences between the calculated geometries for gas phase and adsorbed *cis*-methyl nitrite, only minor differences are found for the calculated vibrational frequencies involving normal modes where there is no direct interaction with the surface. However, when the computed normal frequencies of *cis*-methyl nitrite are compared to those calculated for the *trans*-conformer, significant differences in the N=O and C–O stretching modes and the O–N–O and C–O–N bending modes appear. Therefore, these four modes could be used to discern which of these two conformers can be found on the Au(111) surface. From the calculated results for the adsorbed *cis* species, table 3, it is concluded that only this conformer is present on the Au(111) surface. This conclusion follows from the fact that calculated results for the adsorbed *cis*-conformer compare well with the experimental data and are sufficiently different from those corresponding to the *trans*-conformer. Here, we must mention that for one of the four modes commented above, δ(ONO), the experimental result is in better agreement with the value calculated for the gas phase *trans*-conformer than the corresponding value for *cis*-methyl nitrite. The experimental value, 585 cm^{-1}, is smaller than that corresponding to the gas phase *cis*-isomer and even smaller than that corresponding to the gas phase *trans*-conformer. It is very likely that this normal mode is more affected by lateral interactions which results in the decrease of the ONO angle value, cf. figure 5. In addition, from the proposed adsorption schemes reported in [11], it is difficult to assign the 585 cm^{-1} mode to the adsorbed *trans* species since there are no significant differences involving the location of the oxygen and nitrogen atoms on the silver surface for both the *cis*- and *trans*-conformers.

4. Conclusions

(1) The most favorable adsorption geometry for methyl nitrite on Au(111) is the bridge-bonded central oxygen atom.

(2) The computed structural parameters for the adsorbed species are very close to the gas phase values.

(3) The theoretical value for the adsorption energy is ~33.2 kJ/mol, which compares well with the 33.5 kJ/mol experimental value.

(4) From the vibrational frequency analysis of gas phase and adsorbed species it is concluded that only *cis*-methyl nitrite is present on Au(111), supporting one of the hypotheses proposed in previous studies.

Acknowledgement

This research has been supported by the Spanish DGICYT grant PB98-1216-C02-01 and, in part, by Generalitat de Catalunya grant 1999SGR-00040. JRBG thanks the Fundação para a Ciência e a Tecnologia for a post-doc grant (BPD/22098/99). Part of the computer time was provided by the Centre de Supercomputació de Catalunya, CESCA, and Centre Europeu de Paral.lelisme de Barcelona, CEPBA, through a grant from the Fundació Catalana de la Recerca.

References

[1] A.M. Wodtke, E.J. Jintsa and Y.T. Lee, J. Chem. Phys. 84 (1986) 1044.
[2] G.M. Nazin and G.B. Manalis, Russ. Chem. Rev. 63 (1994) 313.
[3] G.L. Gutsev, P. Jena and R.J. Bartlett, J. Chem. Phys. 110 (1999) 403.
[4] M.J. S Dewar, J.P. Ritchie and J. Alster, J. Org. Chem. 50 (1985) 1031.
[5] S.Y. Hwang, A.C.F. Kong and L.D. Schmidt, J. Phys. Chem. 93 (1989) 8334.
[6] S.Y. Hwang, A.C.F. Kong and L.D. Schmidt, Surf. Sci. 217 (1989) 179.
[7] N. Saliba, J. Wang, B.A. Bausenauer and B.E. Koel, 389 (1997) 147.
[8] J. Wang, B.A. Bausenauer and B.E. Koel, Langmuir 14 (1998) 3255.
[9] J.W. Peck, D.I. Mahon, D.E. Beck and B.E. Koel, Surf. Sci. 410 (1998) 170.
[10] J.W. Peck, D.I. Mahon, D.E. Beck, B. Bausenauer and B.E. Koel, Surf. Sci. 410 (1998) 214.
[11] L.A. Pressley, E.D. Pylant and J.M. White, Surf. Sci. 367 (1996) 1.
[12] J.E. Fieberg and J.M. White, Chem. Phys. Lett. 306 (1999) 103.
[13] D.P. Woodruff, C.F. McConville, A.L.D. Kilcoyne, Th. Lindner, J. Somers, M. Surman, G. Paolucci and A.M. Bradshaw, Surf. Sci. 201 (1988) 228, and references therein.
[14] J.R.B. Gomes and J.A.N.F. Gomes, J. Mol. Struct. Theochem. 503 (2000) 189.
[15] B. Hammer and J.K. Nørskov, Adv. Catal., in press.
[16] P.S. Bagus and F. Illas, in: *Encyclopedia of Computational Chemistry*, Vol. 4, eds. P.V. Schleyer, N.L. Allinger, T. Clark, J. Gasteiger, P.A. Kollman, H.F. Schaefer III and P.R. Schreiner (Wiley, Chichester, 1998) p. 2870.
[17] J.L. Whitten and H. Yang, Surf. Sci. Rep. 24 (1996) 59.
[18] J.R.B. Gomes and J.A.N.F. Gomes, Surf. Sci. 432 (1999) 279.
[19] A. Ricca and C.W. Bauschlicher, J. Phys. Chem. 98 (1994) 12899.
[20] T.V. Russo, R.L. Martin and P.J. Hay, J. Chem. Phys. 102 (1995) 8023.
[21] A. Ricca and C.W. Bauschlicher, Theoret. Chim. Acta 92 (1995) 123.
[22] E.J. Baerends and O.V. Gritsenko, J. Phys. Chem. A 101 (1997) 5383.
[23] P.E.M. Siegbahn and R.H. Crabtree, J. Am. Chem. Soc. 119 (1997) 3103.
[24] A.D. Becke, Phys. Rev. A 38 (1988) 3098.
[25] C. Lee, W. Yang and R.G. Parr, Phys. Rev. B 37 (1980) 785.
[26] R. Colle and O. Salvetti, Theor. Chim. Acta 37 (1975) 329.
[27] R. Colle and O. Salvetti, Theor. Chim. Acta 53 (1979) 55.
[28] P.J. Hay and W.R. Wadt, J. Chem. Phys. 82 (1985) 270.
[29] M.J. Frisch et al., Gaussian 98, Revisions A.5 (Gaussian, Inc., Pittsburgh PA, 1998).
[30] G.L. Gutsev, P. Jena and R.J. Bartlett, J. Chem. Phys. 110 (1999) 403.
[31] B.J. van der Veken, R. Maas, G.A. Guirgis, H.D. Stidham, T.G. Sheehan and J.R. Durig, J. Phys. Chem. 94 (1990) 4029.
[32] P.H. Turner, M.J. Corkill and A.P. Cox, J. Phys. Chem. 83 (1979) 1473.
[33] A.V. de Carvalho, M.C. Asensio and D.P. Woodruff, Surf. Sci. 273 (1992) 381.
[34] M. Bodenbinder, S.E. Ulic and H. Wilner, J. Phys. Chem. 98 (1994) 6441.